

# EXPERIMENTAL MEASUREMENTS AND MODEL PREDICTIONS OF METHYL RADICAL DENSITY IN A DIAMOND MPACVD REACTOR

M. Cappelli<sup>2</sup>, K. Hassouni<sup>1</sup>, T. Owano<sup>2</sup>, X. Duten<sup>1</sup>, and A. Gicquel<sup>1</sup>

<sup>1</sup>Laboratoire d'Ingénierie des Matériaux et des Hautes Pressions

CNRS- UPR 1311, Avenue Jean Baptiste Clément, 93430 Villetaneuse, France

<sup>2</sup>Thermosciences Division, Mechanical Engineering Department, Stanford University, California, 94305-3032

## Abstract

Absolute line-of-sight averaged measurements of methyl radical concentrations in a microwave plasma-assisted diamond deposition reactor are presented. The dependence of the line-of-sight methyl concentration and mole fractions with the percentage of methane in the feed-gas, plasma power density, and position of the substrate relative to the optical probe volume is studied. A comparison is made between the measured mole fractions and predictions based on a one-dimensional diffusive model. The results suggest that the near-substrate methyl mole fraction is influenced by the gas-phase temperature and H-atom density. The measured mole fractions are greater than those predicted by about a factor of ten. This discrepancy is explained in part by the line-of-sight limitations in the experimental facility, and also by the heavy species chemistry involving neutral hydrocarbon species.

## 1. Introduction

The quantitative detection of reactive radicals in hydrocarbon-hydrogen plasmas is important to the understanding of both the gas-phase and surface chemistry during the chemical vapor deposition of diamond. While some measurements of reactive species have been reported in various diamond deposition environments, there are relatively few direct measurements of either atomic hydrogen (H), or methyl radicals (CH<sub>3</sub>), two important reactive species involved in the deposition chemistry, of microwave plasmas<sup>(1,2)</sup>. This is despite the fact that these microwave-sustained plasmas are the most common plasma sources employed in commercial diamond deposition systems. Gicquel *et al.*<sup>(3)</sup> has previously reported on the detection of H by optical emission actinometry in a microwave plasma that has been used extensively to study the synthesis of diamond films. These actinometry measurements were validated in the same reactor by two-photon laser induced fluorescence.<sup>(3)</sup> Furthermore, these measurements provided partial validation of a one dimensional diffusive H<sub>2</sub> + CH<sub>4</sub> plasma.<sup>(3,4)</sup> Experimental and calculated variations of vibration and gas temperatures, as well as relative H-atom mole fraction with percentage of methane, substrate temperature and power density were seen to be in very good agreement.<sup>(2)</sup>

The simulation, based on a model that tracks energy in three separate modes: heavy species translation and rotation, H<sub>2</sub>-vibration, and electron translation, takes into account 29 species and 106 reactions. These latter includes electron impact reactions with H<sub>2</sub> and hydrocarbon

species, heavy species chemistry, as well as ion conversion reactions involving  $H_3^+$  and several hydrocarbon ions.<sup>(4)</sup>

Here, our purpose is to extend the validation of the model to the carbon containing species behavior as function of the plasma variables. We report on the use of ultraviolet absorption for the quantitative detection of methyl densities (densities averaged along a line-of-sight) in the same microwave plasma. The complimentary measurements of H and  $CH_3$  in this plasma reactor will provide a mean for improving validation of the model. The similarities and discrepancies observed between experimental and calculated results are discussed.

## 2. Experimental details

A schematic of the experimental facility is shown in Fig. 1. The microwave plasma has been described in detail in previous papers.<sup>(5)</sup> It consists of a silica bell-jar, in which a feed gas mixture of a few percent methane (0 - 5%) in hydrogen is introduced, and in which a pressure of 18 - 80 mbar is maintained. The particular bell jar used here is equipped with six optical arms on which UV-grade windows are fused. The entire unit is contained within a tunable microwave cavity, connected to a 6 kW, 2.45 GHz microwave generator. Stable plasma operation was achieved at microwave powers of 600 - 2000W. This operating range is typical of that employed in depositing diamond film. The plasma ball, consisting of a sphere of approximately 65-cm<sup>3</sup> in volume at nominal conditions (in the absence of a substrate), was placed in contact with a 5-cm diameter substrate supporting a [100] silicon wafer on which an untextured diamond film had been previously deposited.

Broadband ultraviolet emission from an ultra-stable deuterium lamp (Oriel, Model 63162) is imaged with a magnification of 0.3 using a 100 mm focal length (UV grade silica) lens onto a plane intersecting the center of the plasma ball. The transmitted lamp emission is re-imaged with a magnification of approximately 3 using a second 100-mm focal length lens onto the entrance of a UV-grade silica optical fiber bundle. The line-of-sight of the optical path is passed through the approximate center of the plasma ball, and adjusting the location of the substrate varies the separation between the optical probe and surface. The fiber bundle carries the ultraviolet radiation to the entrance of a Jobin-Yvon (Model Spectrum-1) 0.34m optical multi-channel analyzer, where spectra are recorded using a UV-sensitive 128 (binned) x 1024 pixel CCD array. The monochromator employed an 1800 groove/mm grating blazed at 400 nm. The entrance slit width of the monochromator was set at 0.1 mm. When the grating position was centered at 215 nm, the wavelength range covered by the CCD array extended over 42.9 nm.

The technique used for methyl concentration measurements reported here is similar to that reported in previous papers.<sup>(6,7)</sup> The use of broadband ultraviolet absorption measurements for quantitative detection of methyl radicals in diamond CVD environments was first reported by Childs *et al.*<sup>(8)</sup> A bright source of broadband ultraviolet emission of intensity  $I_{0\lambda}$ , centered about the wavelength of interest,  $\lambda$ , is directed through a plasma containing methyl radicals of number density,  $n_{CH_3}(x)$  that may vary along the line-of-sight direction,  $x$ . The Beer-Lambert law is used to extract the methyl column density from the measured transmitted intensity,  $I_\lambda$ :

$$\int_0^L n_{CH_3}(x) dx = -\frac{1}{\alpha_\lambda(T)} \ln \left( \frac{I_\lambda}{I_{0\lambda}} \right)$$

Here,  $L$  is the dimension of the plasma along the line-of-sight, and  $\alpha\lambda(T)$  is the temperature-dependent ultraviolet spectral absorption cross section. The line-of-sight average methyl density and mole fraction can be expressed in terms of the measured column density as:

$$\bar{n}_{CH_3} = \frac{1}{L} \int_0^L n_{CH_3}(x) dx \quad \bar{\chi}_{CH_3} \approx \frac{k_B T}{PL} \int_0^L n_{CH_3}(x) dx$$

where,  $k_B$  is the Boltzmann constant,  $T$  the gas temperature, and  $P$  the discharge pressure. The expression given above for the methyl mole fraction is valid provided that the gas temperature is not varying significantly along the line-of-sight (that is not the case in this type of plasma). The spectral absorption cross-section can be expressed in terms of the spectral absorption coefficient,  $k\lambda = \alpha\lambda/k_B T$ , which has been measured for methyl radicals.<sup>(7)</sup>

### 3- Model overview

Hydrogen-methane plasmas obtained under diamond deposition discharge conditions exhibit a strong thermal and chemical non-equilibrium. The physical model used here describes the thermal non-equilibrium of these plasmas by taking into account three energy modes : the translation-rotation mode of heavy species ('t-r'), the vibration mode of molecules ('v') and the translation mode of electrons ('e'). The 't-r' and 'v' modes are described by a Maxwell-Boltzmann distribution functions with two different temperatures respectively denoted  $T_g$  and  $T_v$ . Note that in this model, all the molecular species are assumed to have the same vibrational temperature. As far as the 'e' mode is concerned, the electron energy distribution function (EEDF) has been already determined for several discharge conditions by solving the electron Boltzmann equation for the  $H_2/H/CH_4$  system.<sup>(9)</sup> Results showed that for the methane percentage typically used in the considered discharges, the EEDF and related rate coefficients depend very weakly on  $CH_4$  concentration. Furthermore, the electron-heavy species reaction rate constants and the elastic collision frequencies only depend on the electron average energy  $\langle \epsilon_e \rangle$ .<sup>(9)</sup> This result leads to an important simplification when considering the transport modeling of the plasma. As matter of a fact, only an electron average equation is needed for determining the spatial variation of the rates of chemical process and energy transfer. As far as chemistry is concerned, the kinetics model used in this work is similar to that of reference.

<sup>(4)</sup> The chemical non equilibrium of the plasma is described by taking into account 31 chemical species and 134 reactions. The chemical model involves three groups of reactions. The first one corresponds to the chemical model used to describe pure hydrogen plasma.. The second group of reaction describes the thermal cracking of methane and takes into account  $CH_{y=0-4}$  and  $C_2H_{y=0-6}$  neutral species. The third reaction group consists of collisions involving charged species such as electron impact ionization and dissociation of hydrocarbon species, ion conversion processes and dissociative recombination of hydrocarbon ions.<sup>(4)</sup>

The plasma discharge considered in this work is approximated as hemispherical and located just above the substrate so as the whole system is axisymmetrical (Fig. 2). The feed gas flow rate characterizing the deposition experiments are usually very low, i. e. 100-300 sccm, thus resulting in gas flow velocities which are small enough to allow to neglect the convection fluxes with respect to diffusion ones.<sup>(4)</sup> As a consequence, purely diffusive transport was assumed in the present model. Under this assumption and using the thermochemical model described above, the plasma composition and temperatures on the reactor axis are governed by the transport equations given in reference<sup>(4)</sup> coupled to two additional equations which govern the spatial distribution of the absorbed power density. The simulation results presented

in this paper were obtained by solving the non-linear algebraic system resulting from the finite difference formulation of the whole set of transport and power deposition governing equations. The solution method consists of Gauss-Seidel line relaxation technique where the non linear source terms, i. e. chemical production and energy transfer rates, were linearized with respect to species mole fraction and to the temperatures.

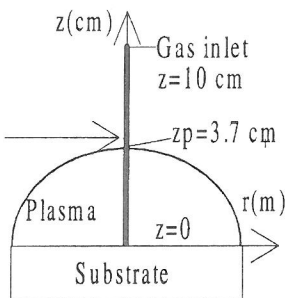
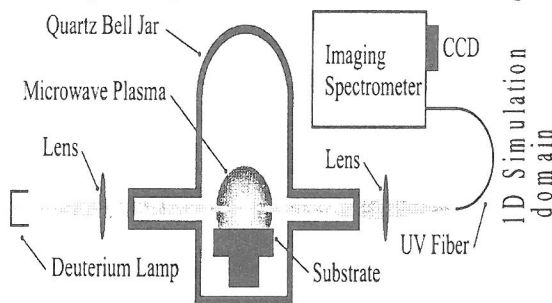


Figure1. Schematic of experimental facility for quantitative detection of methyl in diamond forming microwave plasma.

Fig. 2 : 1D simulation domain and simulation principle

#### 4- Results

At discharge operating at 650W, at a pressure of 18 mbar (1800Pa) (power density of  $8 \text{ W cm}^{-3}$ ), and with 4% methane in hydrogen flowing at  $3.3 \times 10^{-3}$  standard l/sec, an averaged methyl number density of  $1.3 \times 10^{20} \text{ cm}^{-3}$  ( $\pm 15\%$ ) was obtained, given that the gas temperature at this location above the center of the substrate is approximately 1200K<sup>(7)</sup>. The variation in the measured methyl number density with varying methane feed-gas percentage, position in the reactor and power density is shown in Fig. 3 and Fig. 4. In Fig 3, two cases are provided for illustrative purposes: at the same conditions as discussed above, and at conditions of higher power and pressure, with the substrate far from the probe volume (800 W, 40 mbar, i. e. power density of  $12 \text{ W cm}^{-3}$ , 17 mm substrate location,  $T = 2400 \text{ K}$ ). It is apparent that there is a nearly linear relation between the methyl and methane concentration,  $[\text{CH}_3]$  and  $[\text{CH}_4]$ , in the plasma at these two locations and these two power densities. The results from simulations are shown in table 1 for three power densities. A linear relation between methyl and methane concentrations is also apparent.

In figures 3 and 4, also apparent is the increase in the methyl mole fraction (irrespective of the percentage of methane) with increasing power. Figure 5 shows the profile of calculated  $\text{CH}_3$ -radical density along the reactor. A strong decrease in  $\text{CH}_3$  mole fraction in the plasma volume (at 20 mm from the substrate) is observed as the power density increases, while an increase appears in the vicinity of the substrate (2 mm/substrate). The strong decrease in the plasma volume is attributed to the strong increase in the gas temperature with power density (figure 6) that promotes dissociation of  $\text{CH}_3$ , that is displaced towards the production of CH radicals. As observed in table 1, CH radical mole fraction increases (followed by that of  $\text{C}_2$  radicals). At 2 mm from the substrate, due to energy transfer from the plasma to the substrate,  $T_g$  decreases and again favors the formation of  $\text{CH}_3$  radicals (figures 4 and 5).

#### 5- Discussion and conclusion

All the experimental and calculated results are supportive of the conjecture that the methyl radical concentration is tightly coupled to the hydrogen dissociation fraction and to the gas

temperature, in accordance with the nearly partial equilibrium in the hydrogen abstraction reaction:



and that as the fraction of methane is increased, it has little effect on the hydrogen dissociation fraction. Previous studies have also confirmed that variations in the percentage of methane up to 5% has little effect on the atomic hydrogen concentration (see table 1).

An effective production  $\text{CH}_3$  radical from  $\text{CH}_4$  seems then to start at a temperature of around 2000 K, in presence of atomic hydrogen. For temperatures close to 3000 K, the equilibrium set of reactions is displaced toward the production of CH and C species, and  $\text{CH}_3$  radical concentration strongly decreases. Therefore, at low power density,  $\text{CH}_3$  radical concentration is expected to be maximum in the center of the plasma where the gas temperature is maximum. On the contrary, at high power density, we expect the maximum concentration of  $\text{CH}_3$  radical at the vicinity of the surface, where the gas temperature reach 2000 K and atomic hydrogen remains sufficient. As a consequence, while H-atom density at the surface is mainly governed by diffusion process, that of methyl radical is mainly governed by gas phase thermally activated reactions occurring in the close vicinity of the substrate where the gas temperature gradient is controlled itself by diffusion processes.

Although qualitative agreement between experimental and calculated results are observed, an order of magnitude less methyl is experimentally measured than is calculated. Due to the control of  $\text{CH}_3$  radical density by temperature, we expected that line-of-sight averaged measurements include contribution of regions outside the plasma where the production of methyl is probably not negligible. This would result in a overestimate in measured methyl density. Further experiments aimed at obtaining spatially resolved profiles are in progress. Also, gas phase chemistry calculations include 106 reactions, and we cannot exclude the possibility that too many important approximations are made. They could contribute in a systematic error of  $\text{CH}_3$  radical density. A sensitivity study of the mechanism should provide resolution to this possibility.

## 6- Acknowledgments

Olivier Leroy is thanked for his help in modeling and University Paris 13 is thanked for inviting Mark Cappelli and Tom Owano to Paris.

## 7- References

1. D.G. Goodwin and J.E. Butler, in Handbook of Industrial Diamonds and Diamond Films (M. Prelas, G. Popovici, and K. Bigelow, eds), Marcel Dekker, New York, New York (1997), pp. 527-581.
2. A. Gicquel, M. Chenevier, Kh. Hassouni, A. Tserepi, and M. Dubus, J. Appl. Phys. 83, 7504 (1998); A. Gicquel, M. Chenevier, Y. Breton, M. Petiau, J. P. Booth, K. Hassouni, J. Phys III France 6, 1167 (1996); A. Gicquel, K. Hassouni, Y. Breton, M. Chenevier, J.C. Cubertaon, Diamond Relat. Mater. 5, 366 (1996).
3. K. Hassouni, S. Farhat, C. Scott, A. Gicquel, Journal de physique III, 6, 1229-1243 (1996).
4. K. Hassouni, O. Leroy, S. Farhat et A. Gicquel, Plasma Chem. and Plasma Processing, 18 (3), 325 (1998)
5. A. Gicquel, Kh. Hassouni, S. Farhat, Y. Breton, C.D. Scott and M. Lefebvre, and M. Pealat, Diamond Relat. Mater. 3, 581 (1994).
6. M.H. Loh and M.A. Cappelli, Appl. Phys. Lett. 70, 1052 (1997).
7. M. A. Cappelli, T.G. Owano, A. Gicquel, X. Duten, submitted to Plasma Chem. and Plasma Proc.(1999)
8. M.A. Childs, K.L. Menningen, P. Chevako, N.W. Spellmeyer, L.W. Anderson, and J.E. Lawler, Phys. Lett. A 171, 87 (1992).
9. M. Capitelli, G. Colonna, K. Hassouni, A. Gicquel, Plasma Chem. Plasma Process., 16 (2), 153 (1996)

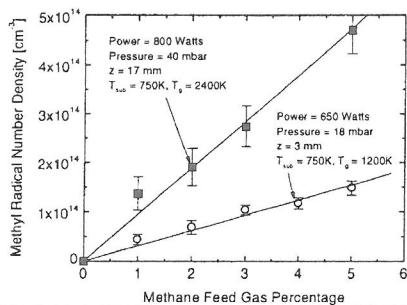


Figure 3 : Variation in the methyl number density with increased methane in the feed-gas.

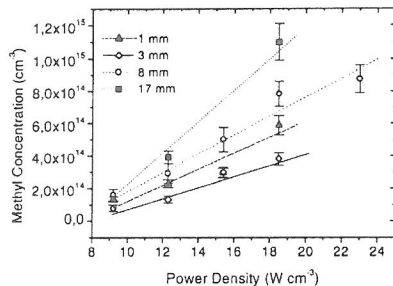


Figure 4 : Variation in the detected methyl number density with increased power density

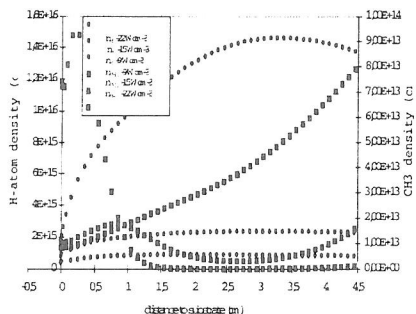


Figure 5 : Variations of  $\text{CH}_3$ -radical and H-atom densities as a function of the distance to the substrate for three power densities. Substrate temperature : 1200 K, 5 %  $\text{CH}_4$ .

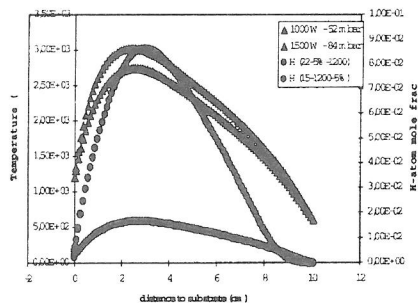


Figure 6 : H-atom mole fraction and gas temperature variations versus the distance to the substrate for two power densities.

9 W cm <sup>-3</sup>		20 mm / substrate				
%CH <sub>4</sub>	x <sub>CH<sub>3</sub></sub> (10 <sup>-04</sup> )	x <sub>CH</sub> (10 <sup>-07</sup> )	x <sub>C<sub>2</sub>H<sub>2</sub></sub>	x <sub>C<sub>2</sub></sub> (10 <sup>-10</sup> )	x <sub>CH<sub>4</sub></sub> (10 <sup>-4</sup> )	x <sub>H</sub>
0	0	0	0	0	0	0.0105
2	2.99	2.96	0.01127	18.4	4.66	0.0099
3	3.28	3.19	0.01717	27.3	5.00	0.0095
5	3.51	3.70	0.02918	49.3	4.8	0.0093
15 W cm <sup>-3</sup>						
%CH <sub>4</sub>	x <sub>CH<sub>3</sub></sub> (10 <sup>-04</sup> )	x <sub>CH</sub> (10 <sup>-07</sup> )	x <sub>C<sub>2</sub>H<sub>2</sub></sub>	x <sub>C<sub>2</sub></sub> (10 <sup>-10</sup> )	x <sub>CH<sub>4</sub></sub> (10 <sup>-4</sup> )	x <sub>H</sub>
0	0	0	0	0	0	0.013
2	0.332	9.06	0.01147	114	0.018	0.017
3	0.341	11.2	0.01665	180	0.015	0.018
5	0.322	17.6	0.0293	428	0.009	0.02
22 W cm <sup>-3</sup>						
5 % CH <sub>4</sub>	x <sub>CH<sub>3</sub></sub> (10 <sup>-04</sup> )	x <sub>CH</sub> (10 <sup>-07</sup> )	x <sub>C<sub>2</sub>H<sub>2</sub></sub>	x <sub>C<sub>2</sub></sub> (10 <sup>-10</sup> )	x <sub>CH<sub>4</sub></sub> (10 <sup>-4</sup> )	x <sub>H</sub>
	8 10 <sup>-3</sup>	67	0.029	5400	2.5 10 <sup>-6</sup>	0.07

Table 2 : Some calculated hydrocarbon mole fractions as function of %  $\text{CH}_4$  and MWPD ( $T_s = 1200$  K).